

# Signal degradation of directly modulated laser by optical fiber dispersion and nonlinearity

Marko M. Krstić, Aleksandar S. Daničić and Dejan M. Gvozdić

**Abstract** – In this paper we investigate the influence of fiber dispersion and nonlinearity on the signal generated by directly modulated laser. We find that fiber dispersion combined with relaxation oscillations of the laser can cause considerable degradation of the signal at the receiver end. This leads to distortion of the eye diagram and narrowing of the eye opening. The nonlinear effects are not so pronounced at low bit rates and short fiber lengths.

**Key words** – laser modulation, relaxation oscillations, fiber dispersion, fiber nonlinearity

## 1. INTRODUCTION

In optical communication systems, intensity modulation is the most common modulation technique. It can be performed externally or directly. The external modulation is based on electroabsorption or Mach-Zehnder modulators, while in direct modulation the output signal is driven by the applied current. In order to make the system simpler and cheaper it is advisable to modulate the laser directly. One of the applications of directly modulated lasers is in "radio-over-fiber" systems. The main flaw of this type of modulation is the occurrence of phenomenon called relaxation oscillations, which may cause signal power degradation and increase of bit-error-rate (BER), even at low bit rates [1]. In this paper, we study the effects of fiber dispersion and nonlinearity on relaxation oscillations and their influence on eye diagram at the receiver end.

Pulse propagation is usually modeled by the nonlinear Schrödinger equation (NLSE) [2], which will be introduced in Sec. 2. in this paper. Sec. 2. also deals with optical gain, rate equations and the nature of relaxation oscillations. The most efficient way of solving NLSE is definitely the *split-step* method, which will be described in Sec. 3. Verification of the numerical method is given in Sec. 4. The results are discussed in Sec. 5. The conclusion of this work is described in Sec. 6.

## 2. THEORETICAL ANALYSIS

In order to get a cheaper optical system, we investigate direct laser modulation. We use  $\text{In}_{0.53}\text{Ga}_{0.47}\text{As}/\text{InP}$  double heterostructure (DH) laser, with active layer thickness of  $d_a = 0.2 \mu\text{m}$  with length and width:  $L = 300 \mu\text{m}$  and  $w = 2 \mu\text{m}$ , respectively. It is assumed that losses in these two layers are  $\alpha_a = 30 \text{ cm}^{-1}$  and  $\alpha_c = 5 \text{ cm}^{-1}$ , respectively.

M. Krstić, A. Daničić and D. Gvozdić are with the School of Electrical Engineering, University of Belgrade, Bulevar kralja Aleksandra 73, 11120 Belgrade, Serbia.

Reflectivities of resonator mirrors are both evaluated to be 0.32, according to the *Fresnel* equations [3]. Electron life time is considered to

be 2.71 ns. The refractive index is calculated to be  $n_{ra} = 3.61$  and  $n_{rc} = 3.32$  for active layer and cladding, respectively. The theoretically ideal model is considered, with no parasitic, and relieved from the effects of the environment.

When a semiconductor laser is modulated, because it takes time for a carrier population  $n$  to build up, there will be a certain time delay before the final photon density  $N_p$  is reached. Once this steady state is achieved, additional time is required for both the carrier (electron-hole pairs) and the photon population to come into equilibrium. This phenomenon, called relaxation oscillations [3], can be simulated by numerically solving the rate equations (1)–(2) [1]:

$$\frac{dn}{dt} = \frac{\eta_i J}{qd} - \frac{n}{\tau} - \Omega \cdot (n - n_{nom}) \cdot \frac{N_p}{1 + \varepsilon \cdot N_p} \quad (1)$$

$$\frac{dN_p}{dt} = \Gamma \cdot \Omega \cdot (n - n_{nom}) \cdot \frac{N_p}{1 + \varepsilon \cdot N_p} + \frac{\Gamma \cdot \theta \cdot n}{\tau_r} - \frac{N_p}{\tau_p} \quad (2)$$

where  $J$  is the injection current density through which we modulate the laser,  $q$  stands for the electron charge and  $d$  is the thickness of the active area.  $\eta_i = \tau_{nr} / (\tau_r + \tau_{nr})$  is the internal quantum efficiency which depends on radiative and nonradiative recombination times  $\tau_r$  and  $\tau_{nr}$ , respectively. Furthermore,  $\tau$  regards to electron lifetime, the differential gain is given by  $\Omega = c/n_r \cdot \partial g / \partial n$  [3] introducing  $g$  as the material gain. Transparency electron concentration is represented by  $n_{nom}$ ,  $\Gamma$  is the optical confinement factor of the active layer,  $\theta$  is the spontaneous emission coupling factor which is defined as the ratio of the spontaneous emission coupling rate due to lasing mode to total spontaneous emission rate [3] and  $\tau_p$  stands for photon life time. For the purpose of obtaining more accurate results and obtaining a realistic model of physical processes in heterostructure lasers, in Eq. (1) and (2) we include nonlinear gain suppression (NGS) coefficient, denoted with  $\varepsilon$ , which has a value of  $2.4 \cdot 10^{-17} \text{ cm}^{-3}$  [4]. More details on solving the system (1)–(2) are given in [1], whereas here we investigate how fiber dispersion and nonlinearities influence the propagation of this signal generated as a solution of (1)–(2).

Maxwell's equations can be used to obtain the wave equation that describes light propagation in optical fibers [2]. The study of most nonlinear effects in optical fibers involves the use of short pulses. When such optical pulses propagate inside a fiber, both dispersive and nonlinear

effects influence their shape and spectrum. In this section we derive a basic equation that governs the propagation of optical pulses in nonlinear dispersive fibers:

$$\nabla^2 \mathbf{E} - \frac{1}{c} \frac{\partial^2 \mathbf{E}}{\partial t^2} = \mu_0 \frac{\partial^2 \mathbf{P}_L}{\partial t^2} + \mu_0 \frac{\partial^2 \mathbf{P}_{NL}}{\partial t^2} \quad (3)$$

where  $\mathbf{E}(\mathbf{r}, t)$  represents the electric field,  $\mathbf{P}(\mathbf{r}, t)$  is induced electric polarization, which consists of two parts such that

$$\mathbf{P}(\mathbf{r}, t) = \mathbf{P}_L(\mathbf{r}, t) + \mathbf{P}_{NL}(\mathbf{r}, t) \quad (4)$$

where  $\mathbf{P}_L(\mathbf{r}, t)$  represents the linear part of the induced polarization, whereas  $\mathbf{P}_{NL}(\mathbf{r}, t)$  is treated as a small perturbation to the total induced polarization. The optical field is assumed to be quasi-monochromatic and able to maintain its polarization along the fiber length so that a scalar approach is valid.

After defining the slowly varying pulse envelope  $A(z, t)$  we can obtain the following equation for pulse evolution inside a single-mode fiber [2]:

$$\begin{aligned} \frac{\partial A}{\partial z} + \frac{\alpha}{2} A + \frac{i\beta_2}{2} \frac{\partial^2 A}{\partial T^2} - \frac{\beta_3}{6} \frac{\partial^3 A}{\partial T^3} = \\ = i\gamma \left( |A|^2 A + \frac{i}{\omega_0} \frac{\partial}{\partial T} (|A|^2 A) - T_R A \frac{\partial |A|^2}{\partial T} \right) \end{aligned} \quad (5)$$

where  $\alpha$  is the absorption coefficient (one can ignore the two-photon absorption coefficient,  $\alpha_2$ , because of its relatively small value for silica fibers),  $\gamma$  is the nonlinear parameter, defined as  $\gamma = (n_2 \omega) / c A_{eff}$ , which, depending on the fiber parameters, takes values in the range of  $10^{-6} - 10^{-5} \text{ (m-mW)}^{-1}$  [2].  $A_{eff}$  is known as the effective core area,  $n_2$  as the nonlinear-index coefficient,  $\beta_2$  represents the effects of chromatic dispersion, while  $\beta_3$  is the third order term in the expansion of  $\beta(\omega)$  in a Taylor series about the carrier frequency  $\omega_0$ , and is generally negligible, as is the case in this paper.  $T_R$  represents the first moment of the nonlinear response function. A frame of reference, moving with the pulse at the group velocity  $v_g$  (so-called retarded frame) is used by making the transformation:  $T = t - z/v_g = t - \beta_1 z$ .

### 3. METHOD

Since the nonlinear Schrödinger equation (NLSE) is a nonlinear partial differential equation, which can be solved analytically only in some specific cases in which the inverse scattering method can be employed, one can conclude that a numerical approach is often necessary for understanding nonlinear effects in optical fibers. Methods used for solving NLSE are the finite-difference methods and pseudospectral methods [2], which are faster than the first ones mentioned. The most frequently used method for solving the pulse-propagation problems in nonlinear dispersive media is the *split-step* Fourier method. This method is much faster since it uses the finite-Fourier-transform (FFT) algorithm.

First we rewrite Eq. (5) in a different form:

$$\frac{\partial A}{\partial z} = (\hat{D} + \hat{N})A \quad (6)$$

where  $D$  is a differential operator that stands for dispersion and absorption in a linear medium and  $N$  is a nonlinear operator that governs the effect of fiber nonlinearities on pulse propagation:

$$\hat{D} = -\frac{i\beta_2}{2} \frac{\partial^2}{\partial T^2} + \frac{\beta_3}{6} \frac{\partial^3}{\partial T^3} - \frac{\alpha}{2} \quad (7)$$

$$\hat{N} = i\gamma \left( |A|^2 + \frac{i}{\omega_0^2} \frac{1}{A} \frac{\partial}{\partial T} (|A|^2 A) - T_R \frac{\partial |A|^2}{\partial T} \right). \quad (8)$$

For the sake of simplicity, we omitted the second and the third term in Eq. (8).

Dispersion and nonlinearity act together along the fiber. The *split-step* Fourier method is actually an approximate solution, in which it is assumed that in propagating the optical field over a small distance  $h$ , the dispersive and the nonlinear effects can be pretended to act independently.

Fiber length is divided into a large number of segments of length  $h$ . Propagation from  $z$  to  $z+h$  is carried out in two steps. In the first one, one can assume that nonlinearity acts alone, and  $D=0$ . In the second step the dispersion acts alone, and  $N=0$ . In the equation

$$A(z+h, T) \approx \exp(h\hat{D}) \exp(h\hat{N}) A(z, T) \quad (9)$$

the exponential operator  $\exp(hD)$  can be expressed in the Fourier domain, by replacing the differential operator  $\partial/\partial T$  by  $i\omega$  where  $\omega$  is the frequency in the Fourier domain. The *split-step* Fourier method is accurate to the second order in the step size  $h$ . The use of the FFT algorithm makes numerical evaluation of Eq. (6) relatively fast. This is the reason why this method can be up to two orders of magnitude faster when compared to most others.

In order to improve this method one can adopt a different procedure to propagate the optical pulse over one segment of the fiber. We assumed again that fiber length is divided into segments of width  $h$ . Now we assume:

$$\begin{aligned} A(z+h, T) \approx \exp\left(\frac{h}{2} \hat{D}\right) \exp\left(\int_z^{z+h} \hat{N}(z') dz'\right) \\ \exp\left(\frac{h}{2} \hat{D}\right) A(z, T) \end{aligned} \quad (10)$$

Now the effect of nonlinearity is not included at the boundaries of the segment, but in the middle. This scheme is known as the symmetrized *split-step* Fourier method [2]. This way, the  $z$  dependence of the nonlinear operator  $N$  is included. The accuracy of this method can be further improved by employing the trapezoidal rule and approximating the integral value in Eq.(8) by

$$\int_z^{z+h} \hat{N}(z') dz' \approx \frac{h}{2} [\hat{N}(z) + \hat{N}(z+h)]. \quad (11)$$

The problem is that the value of  $N(z+h)$  is not known at the point  $z+h/2$ . It is necessary to follow an iterative procedure by replacing  $N(z+h)$  by  $N(z)$ . Then one can estimate the value  $A(z+h, T)$ , which is used to calculate the new value of  $N(z+h)$ .

### 4. VERIFICATION OF THE METHOD

The effective way to test the implemented *split-step* Fourier method is to compare it with the situation when only chromatic dispersion is taken into account. In that case, the fiber transfer function is given by:

$$F(j\omega) = \exp\left(\frac{i}{2} L \beta_2 \omega^2\right) \quad (12)$$

where  $L$  stands for the fiber length. Multiplying this

function with the pulse generated by the transmitter in the Fourier domain, and applying the inverse FFT algorithm on this product, we get the temporal form of the signal at the receiver end of the fiber.

By using the *split-step* Fourier method, we investigate the same signal under the same conditions. Comparison of the obtained results demonstrates the accuracy of the *split-step* method.

In the verification procedure we assume a Gaussian shaped input signal and derive the output signal using both methods explained above. Fig.1 shows four curves: the dotted line represents the input signal, with full width at half maximum of 50ps. The power of the signal is intentionally oversized, in order to show the influence of fiber nonlinearities. The fiber parameters used in this simulation are:  $L = 70$  km as the fiber length,  $\alpha = 0$ ,  $\beta_2 = -2 \cdot 10^{-26}$  s<sup>2</sup>/m and  $\gamma = 0$ . The second and third curves (dark solid lines) are obtained by multiplying the input signal by the transfer function and by using the *split-step* Fourier method, respectively. This is the verification of our numerical method, since these two curves have the exact same shape and completely overlap. The fourth curve (light solid line) shows the complete *split-step* simulation, with  $\alpha = 0$  dB/km,  $\beta_2 = -2 \cdot 10^{-26}$  s<sup>2</sup>/m and  $\gamma = 2.43 \cdot 10^{-6}$  (m·mW)<sup>-1</sup>.

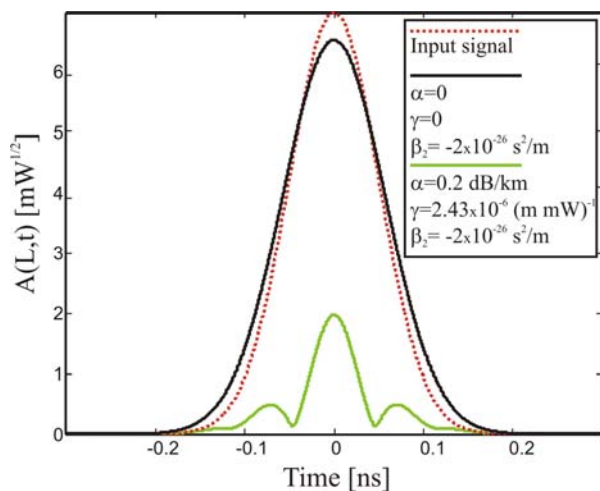


Fig.1. *Split-step* method verification. The curves obtained using two different methods completely overlap.

## 5. RESULTS AND DISCUSSION

The main purpose of this paper is to investigate the influence of fiber dispersion and nonlinearity on directly modulated laser signal. In the case of direct modulation, the signal is affected by relaxation oscillations which cause distortion of the signal and its deviation from the ideal rectangular form. For the sake of comparison, we consider propagation of a rectangular pulse (Fig. 2) and a pulse from a directly modulated DH laser (Fig. 3). The laser parameters are given in Sec. 2.

Fig.2 depicts the ideal rectangular pulse with duration of 0.5 ns. The dashed line represents the input signal, the solid line represents the output signal when only chromatic dispersion is taken into account, while the dotted line

stands for the signal when all three parameters ( $\alpha$ ,  $\beta$ ,  $\gamma$ ) are included. The fiber parameters used in this simulation are the same as in the previous one.

Fig. 3. shows two curves. The dotted one stands for the input rectangular signal affected by the relaxation oscillations, while the solid line represents the signal influenced by the chromatic dispersion only. In the inset, the solid line stands for the same signal as in Fig. 3., and the dotted line represents the signal when  $\alpha$  and  $\gamma$  are also included, with the same values as in Fig. 2.

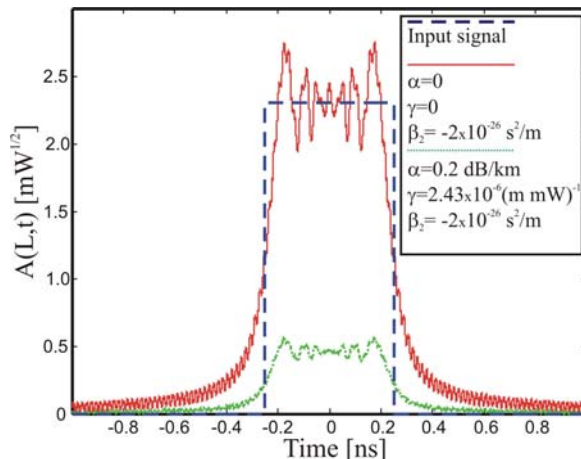


Fig.2. *Input rectangular pulse* (dashed line), *pulse after propagation through fiber, when only chromatic dispersion is included* (solid line) and *pulse after fiber losses and nonlinearity are also included* (dotted line).

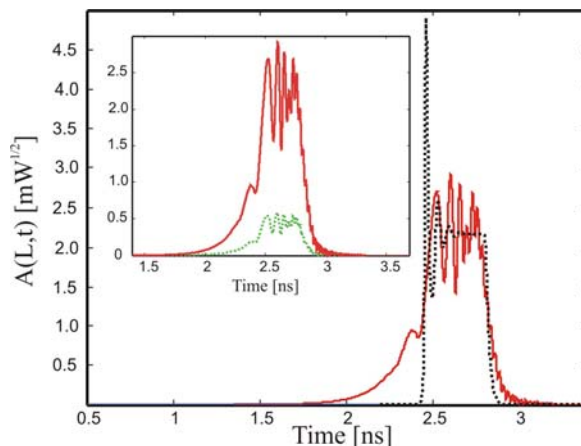


Fig.3. *Directly modulated laser output* (dotted line) and *signal after propagation through fiber, when only chromatic dispersion is included* (solid line). In inset, *solid line stands for the same signal and dotted line represents signal when fiber losses and nonlinearity are also included*.

As it can be seen, the major change in the shape of the input signal is on the horizontal non-zero part of the pulse.

Fig. 4. and Fig. 5. show eye diagrams for rectangular pulse train and for the pulse train generated by the laser. An open eye pattern corresponds to the minimal signal distortion. The distortion of the signal due to relaxation oscillations, dispersion and fiber nonlinearities appears as

closure of the eye pattern.

The eye pattern for dispersion affected rectangular pulse is given in Fig. 4(a). In Fig. 5(a) we present the eye pattern for the laser pulse with relaxation oscillations, affected only by  $\beta_2$ . In Fig. 4(b) and Fig. 5(b)  $\alpha$  and  $\gamma$  are included, with  $\gamma$  intentionally increased, in order to make the influence of nonlinearity more visible. Both eye patterns are obtained for the bit rate of 2.5Gbps.

Relaxation oscillations, combined with fiber dispersion, cause distortion of the eye diagram and narrowing of the eye opening. We find that fiber nonlinearity does not have considerable influence on eye diagrams, at low signal power. When  $\beta_2$  increases, the amplitudes of relaxation oscillations are smaller, but the signal itself broadens, which might lead to an increase of intersymbol interference (ISI) and consequently to an increase of BER. When  $\beta_2$  decreases, the signal broadening is less pronounced, but the ripples of relaxation oscillations are less suppressed. The superposition of the signal ripples and the noise might also lead to an increase of BER. This means that an optimum value for chromatic dispersion coefficient might exist, for which BER, caused by ISI, and the ripples of relaxation oscillations attain a minimum. The influence of these effects on BER will be presented elsewhere.

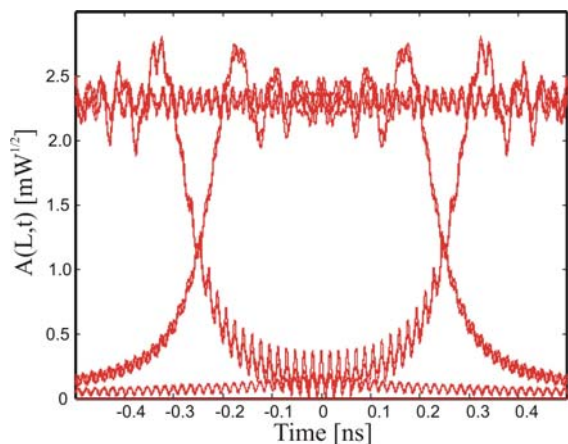


Fig.4.(a) Eye diagram for rectangular pulse for  $\alpha = 0$ ,  $\beta_2 = -2 \cdot 10^{-26} \text{ s}^2/\text{m}$  and  $\gamma = 0$ .

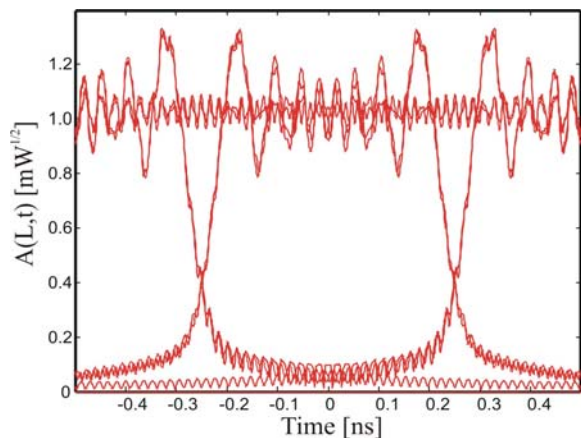


Fig.4.(b) Eye diagram for rectangular pulse for  $\alpha = 0.2 \text{ dB/km}$ ,  $\beta_2 = -2 \cdot 10^{-26} \text{ s}^2/\text{m}$  and  $\gamma = 7.29 \cdot 10^{-6} (\text{m} \cdot \text{mW})^{-1}$ .

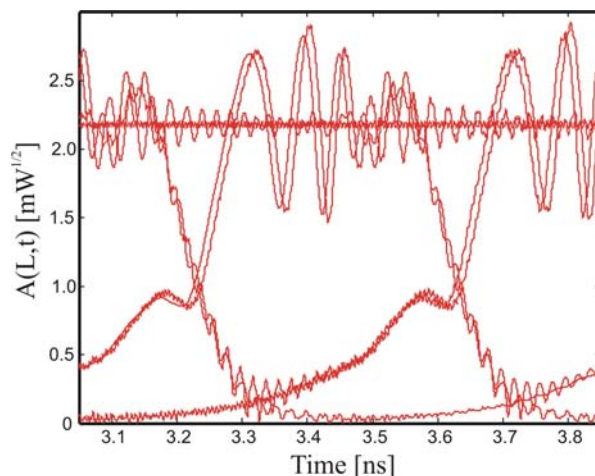


Fig.5.(a) Eye diagram for directly modulated laser output for  $\alpha = 0$ ,  $\beta_2 = -2 \cdot 10^{-26} \text{ s}^2/\text{m}$  and  $\gamma = 0$ .

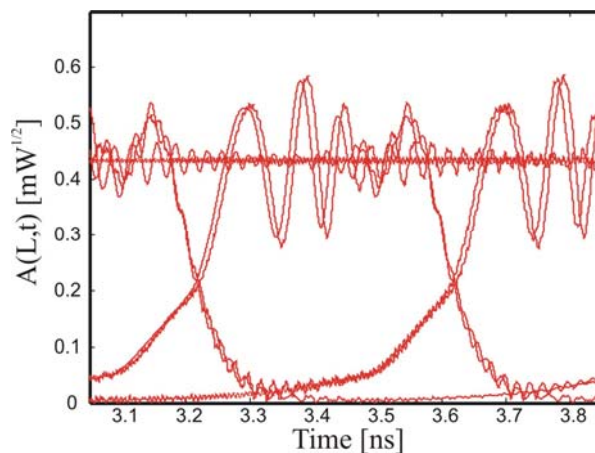


Fig.5.(b) Eye diagram for directly modulated laser output for  $\alpha = 0.2 \text{ dB/km}$ ,  $\beta_2 = -2 \cdot 10^{-26} \text{ s}^2/\text{m}$  and  $\gamma = 7.29 \cdot 10^{-6} (\text{m} \cdot \text{mW})^{-1}$ .

## 6. CONCLUSION

In this paper we analyze the effect of fiber dispersion and nonlinearity on the propagation of directly modulated laser pulses. We calculate the laser response from the rate equations, while the propagation of the laser pulses is simulated by using the Fourier *split-step* method. Our simulation shows that the eye diagram at the receiver end is significantly affected by the ripples of the relaxation oscillations caused by direct modulation of the laser and dispersion effects in the fiber. For low signal powers, nonlinear effects are not as significant.

## 7. REFERENCES

- [1] P. Beliĉev, I. Iliĉ and M. Krstić, "Large signal modulation of semiconductor laser at high bit rates", 51. ETRAN conference, Herceg Novi, 4.-8. june, 2007.
- [2] G. Agrawal, "Nonlinear Fiber Optics", Academic Press, 2001.
- [3] T. Numai, "Fundamentals of Semiconductor Lasers", Springer-Verlag New York, Inc., 2004.
- [4] D.M. Gvozdiĉ and A. Schlachetzki, "Modulation Response of V-Groove Quantum-Wire Lasers", *IEEE J. Quantum Electron.*, vol. 41, pp. 842-847, 2005.